



## Present and Future of Phase-Selectively Disordered Blue TiO<sub>2</sub> for Energy and Society Sustainability

Cite as

Nano-Micro Lett.

(2021) 13:45

Yongguang Luo<sup>1,2</sup>, Hyouyoung Lee<sup>1,2,3,4</sup>

Received: 25 August 2020

Accepted: 18 November 2020

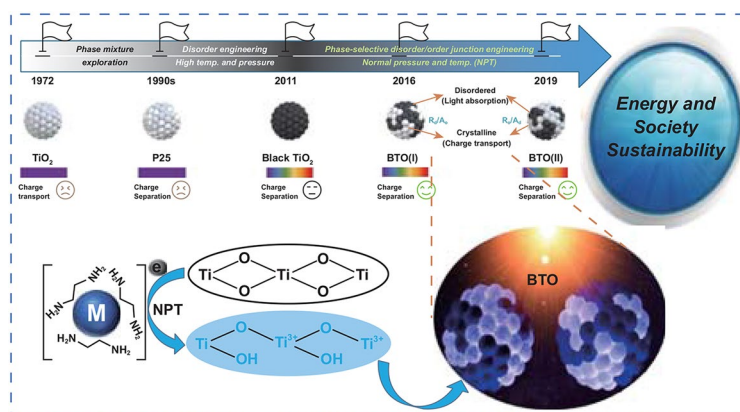
Published online: 4 January 2021

© The Author(s) 2021

### HIGHLIGHTS

- Milestones of TiO<sub>2</sub> development and invention of phase-selectively ordered/disordered blue TiO<sub>2</sub> (BTO) is in-depth illustrated.
- The explored and potential applications of BTO are reviewed and proposed thoroughly.
- The forthcoming flourishing research trends based on account of BTO are suggested.

**ABSTRACT** Titanium dioxide (TiO<sub>2</sub>) has garnered attention for its promising photocatalytic activity, energy storage capability, low cost, high chemical stability, and nontoxicity. However, conventional TiO<sub>2</sub> has low energy harvesting efficiency and charge separation ability, though the recently developed black TiO<sub>2</sub> formed under high temperature or pressure has achieved elevated performance. The phase-selectively ordered/disordered blue TiO<sub>2</sub> (BTO), which has visible-light absorption and efficient exciton disassociation, can be formed under normal pressure and temperature (NPT) conditions. This perspective article first discusses TiO<sub>2</sub> materials development milestones and insights of the BTO structure and construction mechanism. Then, current applications of BTO and potential extensions are summarized and suggested, respectively, including hydrogen (H<sub>2</sub>) production, carbon dioxide (CO<sub>2</sub>) and nitrogen (N<sub>2</sub>) reduction, pollutant degradation, microbial disinfection, and energy storage. Last, future research prospects are proposed for BTO to advance energy and environmental sustainability by exploiting different strategies and aspects. The unique NPT-synthesized BTO can offer more societally beneficial applications if its potential is fully explored by the research community.



Then, current applications of BTO and potential extensions are summarized and suggested, respectively, including hydrogen (H<sub>2</sub>) production, carbon dioxide (CO<sub>2</sub>) and nitrogen (N<sub>2</sub>) reduction, pollutant degradation, microbial disinfection, and energy storage. Last, future research prospects are proposed for BTO to advance energy and environmental sustainability by exploiting different strategies and aspects. The unique NPT-synthesized BTO can offer more societally beneficial applications if its potential is fully explored by the research community.

**KEYWORDS** Blue TiO<sub>2</sub> (BTO); Phase-selective disordering; Visible-light-driven photocatalyst; Charge separation; Energy and society sustainability

✉ Hyouyoung Lee, [hyouyoung@skku.edu](mailto:hyouyoung@skku.edu)

<sup>1</sup> Center for Integrated Nanostructure Physics (CINAP), Institute for Basic Science (IBS), 2066 Seoburo, Jangan-gu, Suwon 16419, Republic of Korea

<sup>2</sup> Department of Chemistry, Sungkyunkwan University, 2066 Seoburo, Jangan-gu, Suwon 16419, Republic of Korea

<sup>3</sup> Creative Research Institute (CRI), Sungkyunkwan University, 2066 Seoburo, Jangan-gu, Suwon 16419, Republic of Korea

<sup>4</sup> Department of Biophysics, Sungkyunkwan University, 2066 Seoburo, Jangan-gu, Suwon 16419, Republic of Korea



## 1 Introduction

Modern society has achieved great science and technology explosion to date but faces severe energy demands and environmental concerns to realize sustainable development. One crucial issue in the twenty-first century is finding ways to convert and store renewable energy efficaciously while tackling climate change and environmental pollution caused by unsustainable human activity. In that context, titanium dioxide ( $\text{TiO}_2$ ) has received a lot of attention for its photocatalytic activity, energy storage capability, low cost, high chemical stability, and nontoxicity. The initial discovery of the photocatalytic potential of  $\text{TiO}_2$  dates back to the end of the 1920s [1]. Researchers observed that aniline dyes faded and fabrics degraded in the presence of  $\text{TiO}_2$ , oxygen gas ( $\text{O}_2$ ), and ultraviolet (UV) light. However, the academic community did not show strong scientific enthusiasm about the phenomenon at that time due to a lack of interest in renewable energy and environmental stewardship.

That began to change after Fujishima and Honda reported the discovery of water photoelectrolysis into hydrogen ( $\text{H}_2$ ) by rutile  $\text{TiO}_2$  under UV irradiation in 1969 [2]. The Honda–Fujishima water splitting finding was refined and called “natural photosynthesis” by *Nature* in 1972 [3]. Now,  $\text{TiO}_2$  is one of the most promising photocatalyst materials. Its valence band (VB) and conduction band (CB) positions offer more diverse catalysis reaction potential than available with many other transition metal oxides and dichalcogenides [4]. Furthermore, the heterogeneous photocatalysis of  $\text{TiO}_2$  enables smoother industrial recycling than is available for homogeneous photocatalysts.

$\text{TiO}_2$  has three main polymorphs, anatase, rutile, and brookite. The anatase and rutile phases of  $\text{TiO}_2$  are the most frequently studied and synthesized in laboratories and industry, whereas brookite, as a natural phase, is rarely investigated as a photocatalyst due to difficulties in synthesizing it [5]. The anatase phase is reported to have higher photocatalytic performance than the rutile phase because it has better bulk charge transportation and a smaller recombination portion of the exciton [6, 7]. After several decades of developments, various  $\text{TiO}_2$  synthesis approaches have been established through gas-phase reactions, solution-based methods, and alcoholysis from titanium tetrachloride ( $\text{TiCl}_4$ ) [8], titanium oxysulfate ( $\text{TiOSO}_4$ ) [9], and  $\text{Ti}(\text{OC}_4\text{H}_9)_4$  [10]. To date, one of the famous  $\text{TiO}_2$  photocatalyst products is

commercial Degussa P-25 (P25) (Degussa Co., Ltd), which has been frequently applied as a benchmark photocatalyst [11, 12]. P25  $\text{TiO}_2$  contains a unique hybrid of anatase and rutile phases in a roughly 3:1 ratio and exhibits good performance in many photocatalytic systems [13].  $\text{TiO}_2$  is also used in other industries: energy (energy production and storage), environment (degrading pollution in the air, wastewater, and indoors), human health and food (antibacterial, anti-virus sterilization), cosmetics (sunscreen against UVA and UVB), and self-cleaning and antifogging products [14, 15]. The antiviral potential of  $\text{TiO}_2$  will certainly draw attention during the struggle with the COVID-19 coronavirus pandemic [16].

$\text{TiO}_2$  still faces several hindrances to its photocatalytic performance. First, pristine  $\text{TiO}_2$  can absorb sunlight only in the UV region (5%) due to its large electronic bandgaps (anatase, 3.2 eV; rutile 3.0 eV), which results in extremely low photocatalysis quantum efficiency that fails to meet the needs of industrial applications. Second, the separated charges (electrons and holes) formed after photoexcitation of a photocatalyst can recombine and disappear, giving subsequent photoluminescence. This exciton recombination process reduces the number of active electrons and holes on the photocatalyst surface, which is detrimental to any photocatalysis reaction. Therefore, research is needed to boost light absorption efficiency and block charge recombination to maintain a high exciton dissociation capability. Many attempts have been made to attain a broader range of light absorption by using non-metallic elements (C, N, and S) [17] and transition metal doping [18, 19] to tune the  $\text{TiO}_2$  electronic structure. However, only a few researchers have tried to develop advanced  $\text{TiO}_2$  by targeting both visible-light absorption and high charge separation efficiency. Those efforts produced “Black  $\text{TiO}_2$ ” [20] and “Blue  $\text{TiO}_2$ ” [21] in 2011 and 2016, respectively. In addition, the phase-selectively disordered blue  $\text{TiO}_2$  (BTO) offers high  $\text{H}_2$  generation performance through its three unique phase–interface configurations.

Next, we summarize several historical milestones in the development of  $\text{TiO}_2$  materials and then systematically illustrate the development logic and discovery of BTO, including its mild synthesis conditions, robust reducing agent design, and phase-selective disordering. The phase selectivity of BTO results from its unique structure, which we disclose on the crystalline dimension level, and the reduction power of alkali metal amines. Its ordered-disordered phase

junctions, type II band alignment structure, and a surface rich in hydroxyl groups explain the high exciton dissociation efficiency, visible-light absorption, and superior photocatalysis of BTO. Particularly, we further present the exploratory attempts of BTO in various energy and environmental aspects. Finally, we suggest future research avenues to explore the potential of BTO further.

## 2 Milestones in TiO<sub>2</sub> and the Development of BTO

The research community has long worked to exploit the energy efficiency and activity of TiO<sub>2</sub> in versatile applications. Events of considerable significance in the recent history of TiO<sub>2</sub> development are shown in Fig. 1a. The first fundamental finding in TiO<sub>2</sub> photocatalysis for energy conversion was a report of water electrochemical photolysis which generates the absolute clean energy gas, H<sub>2</sub>, using a rutile TiO<sub>2</sub> semiconductor electrode in 1972 by Fujishima and Honda et al. However, the applied rutile TiO<sub>2</sub> has lower charge transportability than anatase TiO<sub>2</sub>, even though it has better light absorption efficiency to generate more charges. The underlying reasons that anatase has better charge transportation than the rutile phase are the higher VB maximum energy level of the anatase phase (Fig. 1b) [7], its preferred crystalline surface orientation [22], and its longer exciton (electron and hole pair) lifetime [23]. To use the advantages of both the anatase and rutile phases, the commercially available phase-mixed P25 TiO<sub>2</sub> has been widely used as a standard photocatalyst. It has been proved a better activity than the single-phase TiO<sub>2</sub> since the 1990s [13, 24, 25]. Extending the TiO<sub>2</sub> light absorption range was the main challenge after the development of P25. In 2011, Xiaobo Chen et al. found that TiO<sub>2</sub> phase disorder engineering through hydrogenation enhanced its light absorption capability into the visible and infrared ranges [20]. That hydrogenated black TiO<sub>2</sub> mostly answered concerns about the photocatalysis energy efficiency of TiO<sub>2</sub>. Moreover, the photocatalytic activity of black TiO<sub>2</sub> is boosted by suppressing exciton recombination through the middle VB by means of localized holes generated in the disordered surface. During approximately four decades of research, TiO<sub>2</sub> material development has produced decent UV–visible-light absorption, acceptable photocatalytic activity, and reasonable charge generation. Nevertheless, TiO<sub>2</sub> still requires

more development to be practical for energy production and photocatalysis applications. After thoroughly investigating the recent achievements in black TiO<sub>2</sub> material design, we found that most black TiO<sub>2</sub> synthesis approaches require high temperatures (400–900 °C) or a high H<sub>2</sub> atmospheric pressure (20–70 bar) [26]. Furthermore, the black TiO<sub>2</sub> core/shell structure produces a back reaction that diminishes its photocatalytic power because of its sole surface reaction interface. The issues that remain to be addressed since the development of black TiO<sub>2</sub> are developing an industrially suitable manufacturing process with mild conditions and further strengthening exciton dissociation and catalytic reaction efficiency.

## 3 NPT Synthesis of BTO and Its Phase-selective Specialty

The high-temperature and H<sub>2</sub> atmospheric pressure synthesis conditions of most black TiO<sub>2</sub> are energy-intensive and potentially explosive, an unfavorable manufacturing choice in both laboratories and industry. Therefore, it is essential to find a suitably, potent reducing agent or system. Birch reduction agents, an alkali metal in liquid ammonia, can reduce arenes into cyclohexadiene rather than cyclohexane [27]. Among the Birch reduction processes, the electride salts that form by mixing an alkali metal (M) and ammonia (NH<sub>3</sub>) as [M(NH<sub>3</sub>)<sub>x</sub>]<sup>+</sup> e<sup>-</sup> have strong reducing power. Therefore, we supposed that producing such vital electride salts as a reduction species would contribute to TiO<sub>2</sub> reduction. We found that a lithium ethylenediamine (Li-EDA) solution reduced the rutile phase of P25 TiO<sub>2</sub> while keeping the anatase phase intact, which resulted in a unique blue TiO<sub>2</sub> product (BTO(I)) [21].

The superior photocatalysis performance of BTO stimulated us to investigate the origin of its phase selectivity further. As shown in Fig. 2a, the free electron of M-EDA electrides can attack the firm Ti–O bond and produce a reduced Ti<sup>3+</sup> state. The evidence for Ti<sup>3+</sup> and oxygen vacancy (OV) were provided by X-ray photoelectron spectroscopy and electron paramagnetic resonance in our previous reports from 2015 to 2019, respectively. Besides, the reduced TiO<sub>2</sub> is generally presented in a disordered amorphous physical state with a black appearance. The blue color of BTO is caused by the coexistence of an ordered crystalline anatase (A<sub>o</sub>) phase and a disordered amorphous rutile (R<sub>d</sub>) phase.



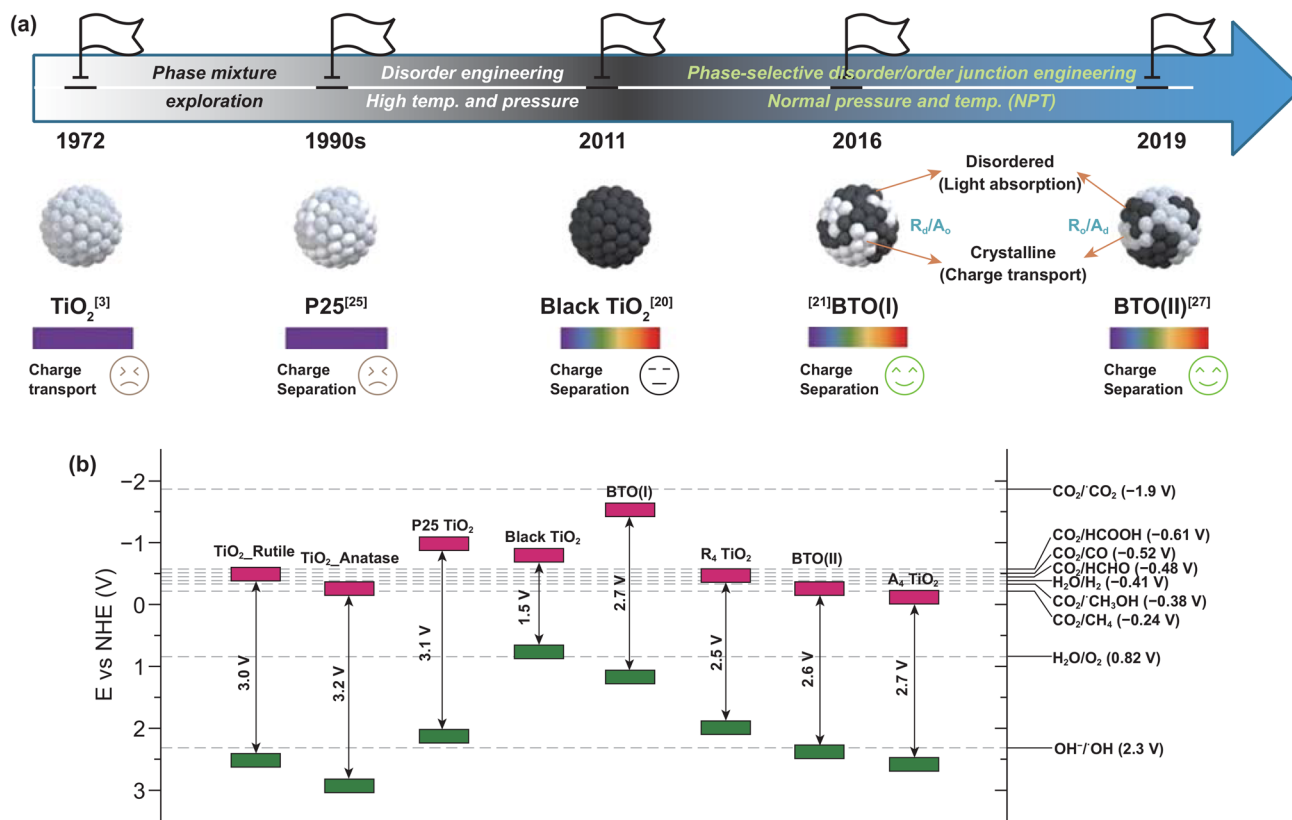


**Fig. 1** **a** Milestones in  $\text{TiO}_2$  material development and **b** the corresponding band structure of each typical  $\text{TiO}_2$  configuration [3, 20, 21, 25, 28, 32]. The  $\text{TiO}_2$  nanoparticles illustration figures in **(a)** are adapted with the permission from Ref. [28]. Copyright (2019) American Chemical Society

The successful reduction of  $\text{TiO}_2$  by a Li-EDA solution in normal pressure and temperature (NPT) conditions indicates its mighty reducing power. It successfully replaced the high pressure and temperature hydrogenation reduction approach.

After successfully preparing ordered anatase ( $A_0$ )/disordered rutile ( $R_d$ )  $\text{TiO}_2$  from P25 with the Li-EDA solution under NPT conditions, we set out to design disordered anatase ( $A_d$ )/ordered rutile ( $R_o$ )  $\text{TiO}_2$  from P25. With the curiosity of other alkali metal EDA reduction phenomena, we applied Na and K EDA solutions to reduce the P25. Interestingly, the Na/K-EDA solution selectively reduced the P25  $\text{TiO}_2$  reverse from the Li-EDA. Figure 2b shows that P25  $\text{TiO}_2$  turns to  $R_d/A_o$  (BTO(I)) through Li-EDA reduction and  $R_o/A_d$  (BTO(II)) through Na/K-EDA reduction. Furthermore, the anatase and rutile phases  $\text{TiO}_2$  were individually treated by Li-EDA and Na/K-EDA, respectively. The pure white rutile  $\text{TiO}_2$  becomes black  $R_d$   $\text{TiO}_2$  in a Li-EDA environment, and the anatase single-crystalline form becomes black or gray  $A_d$   $\text{TiO}_2$  after

the Na/K-EDA reduction. Based on that initial finding, which we were the first to report, the  $\text{TiO}_2$  architecture can be widely enriched to extend its potential applications. Because of their blended ordered and disordered phase structure, BTO(I) and BTO(II) have high potential as photocatalysts with effective heterojunctions and visible-light absorption. In addition, the M-EDA-reduced  $R_d$  and  $A_d$  can be used to anchor hybrid material systems and maintain a steady structure through covalent combinations.

To investigate the best amines for dissolving alkali metals and reducing  $\text{TiO}_2$ , we selected various liquid amine derivatives, including monoamines with different alkyl chain lengths (Numb. 1–4 in Fig. 2c) and diamines with diverse alkyl chain lengths and positions (Numb. 5–8 in Fig. 2c). The various M-amine solutions produced diverse forms from the P25 that were colored from blue to gray. Among them, the shortest alkyl chain diamine solution, Na-EDA, exhibited the best reduction results, producing a deep blue color and entirely vanished anatase crystalline phase, as shown in the

detailed XRD characterization in Ref. [28]. EDA's effects result from its effective diamine structure and higher polarity than the long alkyl chain amines, which contribute to its high alkali metal solubility. This newly developed, powerful reducing system (M-EDA) can be readily extended to the reduction of other metal oxides or metal sulfides and defect design objectives.

Next, we examined the crystallography of anatase and rutile  $\text{TiO}_2$  at the atomic level to find the origins of the phase selectivity. Beginning with facet information about the rutile (110) and anatase (101) phases [28–30], we found the gap distance in the unit lattice to be around  $2.96 \text{ \AA} \times 2.96 \text{ \AA}$  for rutile (110) and  $2.86 \times 3.79 \text{ \AA}^2$  for anatase (101), as shown in Fig. 2d. The diameters of Li, Na, and K atoms in the EDA environment are 2.7, 3.1, and 3.9  $\text{\AA}$ , respectively, as shown in the inserted table in Fig. 2d. Clues about phase selectivity

can be drawn from that lattice and atomic size information. Na and K, which are larger than Li, are relatively close to the anatase (101) lattice unit dimensions but more massive than the rutile (110) lattice gaps. Therefore, Na and K can attack Ti–O–Ti bonds in the anatase phase and break the anatase crystalline into a disordered state. On the other hand, Li atoms can effectively attach to the rutile (110) lattice units, rather than the wider lattice spaces of the anatase (101), and thus successfully reduce only the rutile  $\text{TiO}_2$  phase. In that way, the intrinsic adaptability of Li-EDA to the rutile phase and Na/K-EDA to the anatase phase determine the selectivity of the disordering results.

Furthermore, the M-EDA treatment process is easy to scale up and highly repeatable through the alkali metal stepwise feeding. Using a hydrophilic material is necessary to provide good interfacial contact in many photocatalysis

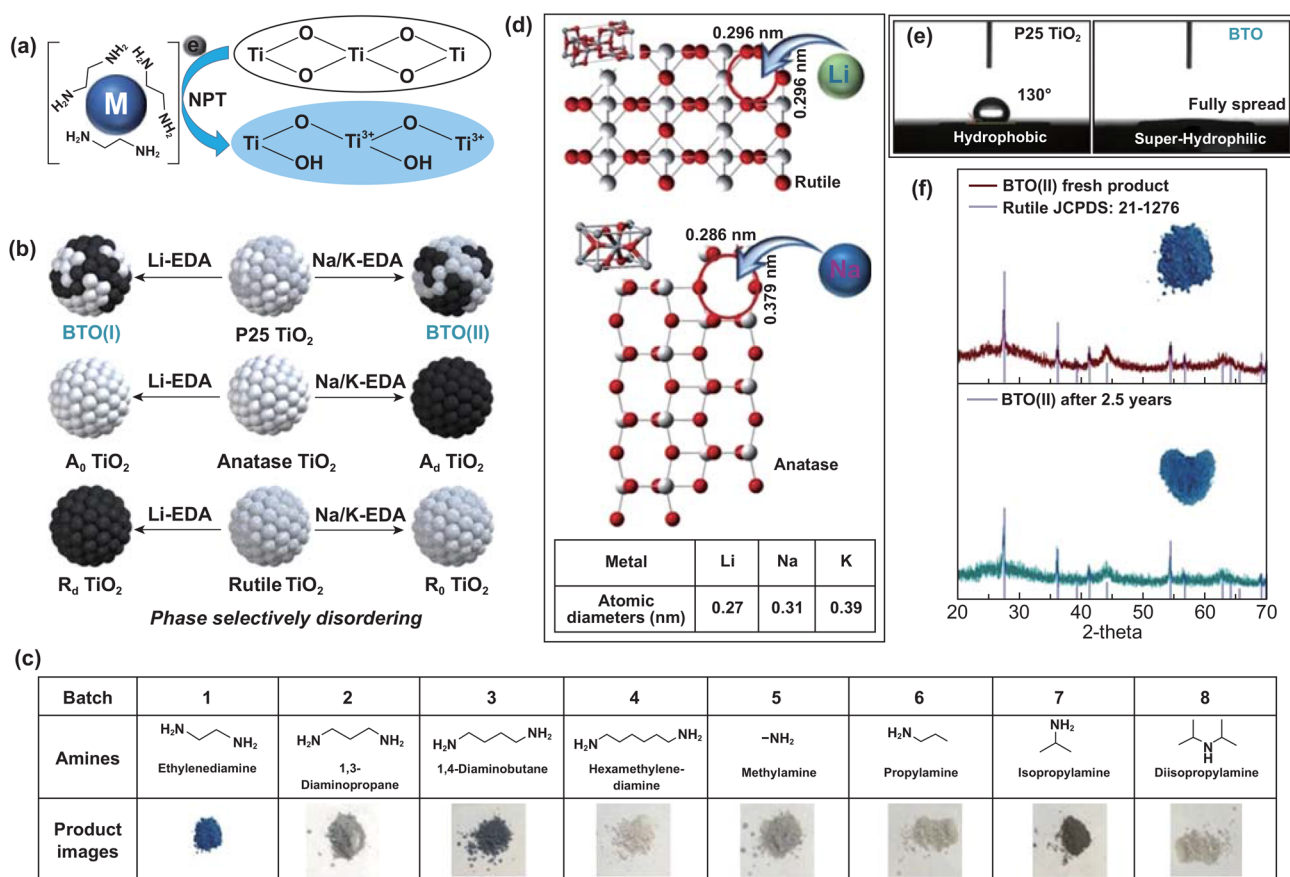


**Fig. 2** NPT synthesis of BTO and its phase selectivity. **a** M-EDA electrifies reduce pristine  $\text{TiO}_2$  to BTO under NPT conditions. **b** Different starting  $\text{TiO}_2$  phases are selectively reduced/disordered by M-EDA solutions. **c** Amine solvent investigation to synthesize BTO. Adapted with permission from Ref. [28]. **d** Proposed mechanism for the BTO phase-selective phenomenon. Adapted with permission from Ref. [28, 29]. **e** Water contact angle measurements (SEO PHX300) of the original P25  $\text{TiO}_2$  and the phase-selectively reduced BTO. **f** Structure and appearance stability characterization by X-ray powder diffraction (SmartLab JD3643N) and digital photo images

and other real-world applications. As shown in Fig. 2e, a water drop fully spreads on the BTO film, which indicates that BTO is more hydrophilic than pristine P25 TiO<sub>2</sub>. The excellent hydrophilicity of BTO originates from the enriched surface hydroxyl (OH) groups that appear after the M-EDA reduction. Pristine P25 TiO<sub>2</sub> has a hydrophobic surface, with a 130° water contact angle, due to the absence of hydrophilic functional groups on its intact TiO<sub>2</sub> surface. Material stability is another concern for practical applications. BTO has maintained its original disordered/ordered structure and appearance for almost 2.5 years under ambient conditions, as represented in Fig. 2f. Thus, BTO has many advantages, from low-cost production to high potential for many practical applications.

## 4 Explored and Potential Applications of BTO

BTO exhibits strong visible-light (380–740 nm) absorption ability with a narrow optical bandgap (Fig. 1b), efficient photoinduced exciton disassociation with a heterojunction structure [21], and excellent hydrophilicity and stability (Fig. 2e, f). Our group has applied BTO to promote green energy and social sustainability in the field of hydrogenation [21], algae elimination from aquatic ecosystems [31], carbon dioxide (CO<sub>2</sub>) reduction [28, 32], and visible-light-driven organic synthesis (C–H arylation) [33]. Next, we describe those BTO applications and then propose strategies and directions for further designs and applications of BTO.

### 4.1 Explored Photocatalytic Aspects of BTO

Hydrogen has been deemed a perfect blue energy source that could solve the energy crisis in the twenty-first century. For example, its heating value (141.72 MJ kg<sup>-1</sup>) is three times higher than gasoline (46.4 MJ kg<sup>-1</sup>) [34], and it is an extremely abundant material that produces zero pollution and has reproducible capabilities through the water. Solar-driven photohydrogenation has received much attention because of its high sustainability. BTO, as a typical semiconductor material, can be used as a robust hydrogenation photocatalyst and has shown a remarkable performance enhancement over P25 and most other reported TiO<sub>2</sub> materials [21]. The extended light absorption spectrum of BTO covers all solar illumination, which maximizes the quantum

efficiency of its photocatalysis process. However, it is not enough to have a favorable light-harvesting ability; a desirable hydrogenation photocatalyst must also produce effective charge separation through a specific structure designation. As shown in Fig. 3a, BTO retains discrete catalytic redox reaction sites for the reduction of water to hydrogen and methanol sacrificial agent oxidation. The right-side gray R<sub>d</sub> is responsible for absorbing enough light irradiation and generating the photoinduced electron and holes. Afterward, the adjacent A<sub>o</sub> accepts electrons to trigger water splitting. Compared with the conventional core–shell structure of black TiO<sub>2</sub>, BTO eliminates the need for electrons to migrate from the core to the interface of the shell and water. Therefore, it greatly reduces the potential for charge recombination. Furthermore, the type II band alignment configuration of BTO assists in exciton dissociation and keeping the effective charges. The open ordered/disordered structure of BTO realized a superior H<sub>2</sub> production rate of 13.89 mmol h<sup>-1</sup> g<sup>-1</sup> with 0.5 wt% Pt and 3.46 mmol h<sup>-1</sup> g<sup>-1</sup> without the Pt co-catalyst.

Algae blooms happen regionally in various brine and river systems, mainly due to water eutrophication induced by human activities, and they damage public health and the social economy [35]. Severe overgrowth of algae can kill aquatic creatures by consuming the limited oxygen dissolved in the water. TiO<sub>2</sub>, as a typical photocatalyst, can generate reactive oxygen species (ROS), which mainly consist of a hydroxyl radical (·OH) and superoxide anion radicals (·O<sub>2</sub><sup>-</sup>), through photo irradiated hot carriers that attack water molecules. The ROS then remove algae. However, conventional TiO<sub>2</sub> has low efficiency in generating sufficient ROS for algae elimination. Based on our previously obtained photocatalytic hydrogenation experience, we applied BTO to remove *Chlamydomonas* green algae (Fig. 3b) [31]. We expected that the powerfully wide range of light absorption and effective charge separation properties of BTO would produce an efficient ROS amount. The algae removal test was conducted under both UV and solar light with various types of TiO<sub>2</sub>. The BTO wiped out all the algae cells within 2–2.5 h, which was the most rapid among the kinds of TiO<sub>2</sub> tested. Thus, BTO has meaningful roles to play in realizing a sustainable society.

The photoreduction of CO<sub>2</sub> into chemical fuels under solar or visible light is supposed to be an excellent way to target both energy and environmental concerns. This so-called artificial photosynthesis strategy has been under

study for a while, but desirable conversion selectivity and production yield are still lacking [36]. Moreover, it is quite hard to crack the C=O bonds in the CO<sub>2</sub> molecule because the dissociation energy demand is high (around 750 kJ mol<sup>-1</sup>) [37]. The ideal photocatalyst for the CO<sub>2</sub> reduction reaction (CO<sub>2</sub>RR) needs a specific configuration with an optical band position (especially the CB) that is close to the CO<sub>2</sub> reduction potential, such as the  $-0.24 V_{\text{NHE}}$  of CO<sub>2</sub> to CH<sub>4</sub> or the  $-0.52 V_{\text{NHE}}$  of CO<sub>2</sub>/CO, and also efficient charge separation with good electron transport. BTO has those structures, so we conducted CO<sub>2</sub> reduction experiments using BTO(II) under visible light [28] and BTO hybrid materials (BTO(I)/WO<sub>3</sub>-Ag) under solar light [32]. The BTO(II) reached unprecedented CH<sub>4</sub>

production levels (3.98 μmol g<sup>-1</sup> h<sup>-1</sup>), with the highest yield among all the metal (Pt, Ru, W, and Ag)-doped P25 TiO<sub>2</sub> materials tested. The evident CO<sub>2</sub>RR ability was conferred by the excellent match between the CB position of BTO(II) ( $-0.24 V_{\text{NHE}}$ ) and the CO<sub>2</sub> to CH<sub>4</sub> potential and the efficient visible-light absorption by the A<sub>d</sub> with rapid charge-carrier disassociation (Fig. 3c). Even though BTO(II) offered excellent CO<sub>2</sub>RR performance, another critical issue for CO<sub>2</sub>RR, product selectivity, also has to be addressed. Consequently, we designed and constructed BTO(I)/WO<sub>3</sub>-Ag, a combination material intended to build a particular Z-scheme band structure, as presented in Fig. 3d. The assembled Z-scheme band alignment can maximize the effective potential between a high CB and

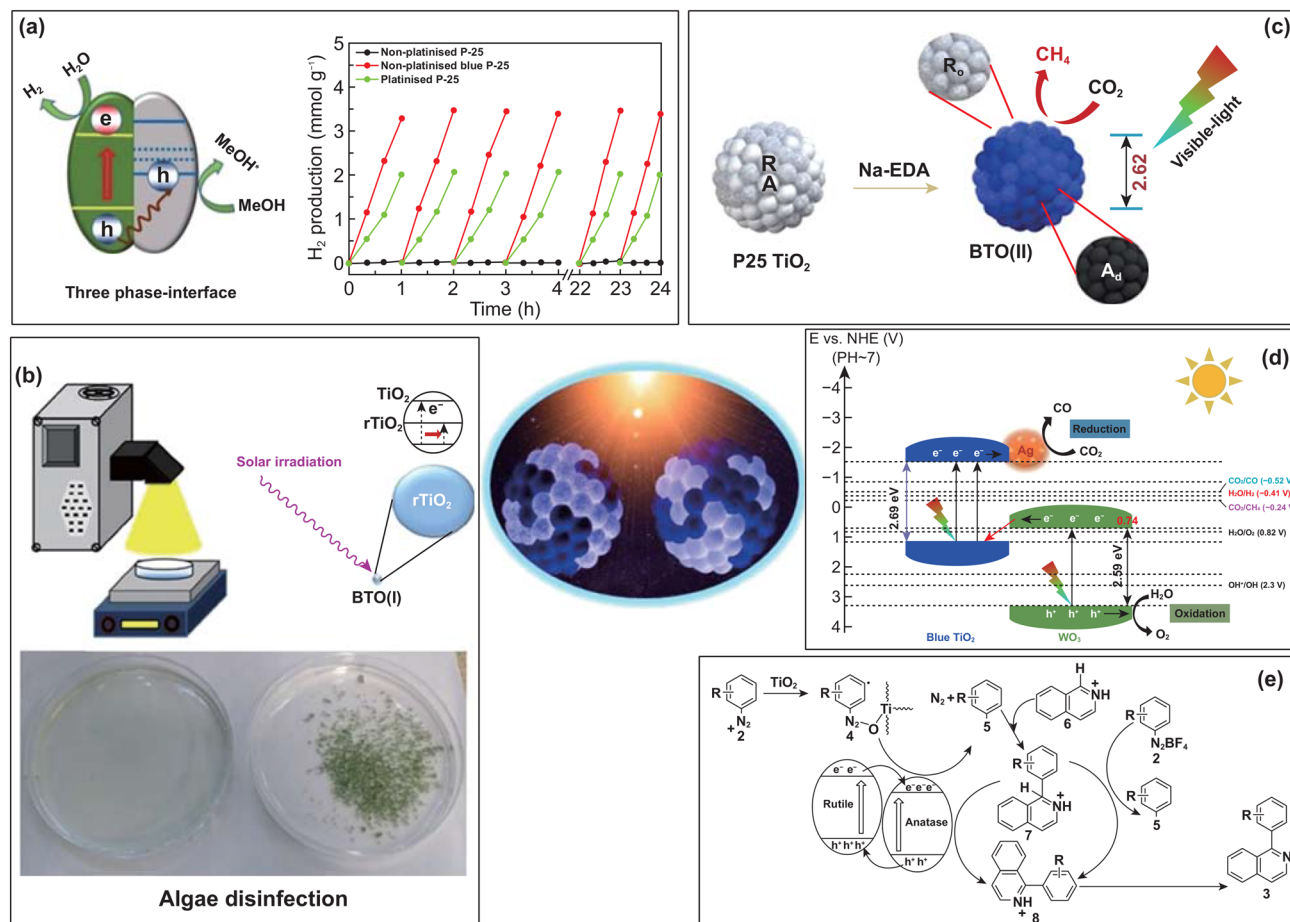


**Fig. 3** Explored photocatalytic applications for BTO. **a** Unique three-phase-interface BTO(I) robust H<sub>2</sub> photogeneration from water. Adapted with permission from Ref. [21]. **b** Efficient *Chlamydomonas* green algae disinfection by BTO(I) under solar irradiation. Adapted with permission from Ref. [31]. **c** Visible-light-driven CO<sub>2</sub> reduction (CO<sub>2</sub>RR) to CH<sub>4</sub> by BTO(II). Adapted with permission from Ref. [28]. **d** BTO(I)/WO<sub>3</sub>-Ag combination with a Z-scheme band structure for high-selectivity CO<sub>2</sub>RR to CO. Adapted with permission from Ref. [32]. **e** BTO(I) photocatalytic activity in C-H arylation organic synthesis. Adapted with permission from Ref. [33]

low VB and then strengthen the catalytic redox power. Notably, the CB position ( $-1.55 V_{\text{NHE}}$ ) of BTO(I) is close to the  $\text{CO}_2$  to CO potential (Fig. 1b), which contributes to CO production, and higher than the CB of  $\text{WO}_3$  ( $0.74 V_{\text{NHE}}$ ) used to construct the Z-scheme band alignment. In addition, the low difference between the VB of BTO(I) ( $1.14 V_{\text{NHE}}$ ) and the CB of  $\text{WO}_3$  facilitates the flow of excited  $\text{WO}_3$  electrons to BTO(I), thereby reinforcing the number of effective hot electrons. The decorated Ag nanoparticles serve as an electron reservoir that can initiate photoelectron production by means of the localized surface plasmon resonance effect and further enhance visible-light absorption. When tested, this BTO based Z-scheme composite produced absolute CO selective-production of  $1166.7 \mu\text{mol g}^{-1} \text{h}^{-1}$  at the excellent photocatalytic electron reaction pace of  $2333.4 \mu\text{mol g}^{-1} \text{h}^{-1}$ . All in all, BTO showed vigorous  $\text{CO}_2\text{RR}$  strength in producing  $\text{CH}_4$  or CO with high output and selectivity, which means it can be an attractive way to tackle global warming and energy deficiency together.

Light-driven chemical synthesis is also an essential field that requires promising photocatalysts to boost synthesizing efficiency [38]. C–H arylation for organic synthesis was chosen as a typical study case to show the photocatalytic activity of BTO (Fig. 3e) [33]. The phase-mixed BTO absorbs light in the visible range through its  $\text{Ti}^{3+}$  defect-rich disordered state. It maintains good adsorptivity of an organic reactant and charges separation via its ordered crystalline phase. First, a charge transfer complex (4) formed on the  $A_0$  site of BTO(I) from the aryl diazonium compound (2). Then, under visible-light irradiation, photogenerated electrons flowed to the anatase CB due to the type II band alignment and efficiently separated from the holes. An aryl intermediate radical (5) was produced after the single electron transfer process from  $A_0$  to (4). As arylation proceeded, after initiation by aryl radical (5), the resulting radical (7) intermediate was oxidized by the hot hole carrier from the  $A_0$  VB and gave the desired product (3) after deprotonation of the product (8). Moreover, BTO offers high reusability through direct filtration, and it maintained consistent yield (63%) performance when five batches were examined under six-fold scaled-up conditions. This application of BTO to photocatalytic chemical synthesis will enrich the role of  $\text{TiO}_2$  in industrial chemical synthesis and contribute to further product cost reductions.

## 4.2 Potential Application and Design Commentary of BTO

Currently, ammonia ( $\text{NH}_3$ ) synthesis from nitrogen gas ( $\text{N}_2$ ) is an essential approach to supplying nitrogen to plants and humans by industry manufacturing. The Haber–Bosch process for  $\text{NH}_3$  synthesis ( $\text{N}_2 + \text{H}_2 \rightarrow \text{NH}_3$ ), which has been used in industry for more than a century, urgently needs to be replaced due to its high consumption of fossil fuels, which results in enormous greenhouse gas ( $\text{CO}_2$ ) emissions and extremely harsh operating conditions ( $400\text{--}500^\circ\text{C}$ ,  $100\text{--}200$  bar with an iron-based catalyst) [39]. Therefore, photocatalysis nitrogen fixation that can use sustainable solar energy and eliminate  $\text{CO}_2$  emissions has attracted growing attention. However, it remains challenging to design an efficient photocatalyst to convert  $\text{N}_2$  to  $\text{NH}_3$  under NPT conditions with a high production rate and clear mechanism [40]. It has been reported since 1977 that  $\text{TiO}_2$  generated  $\text{NH}_3$  and other gasses under UV irradiation with an  $\text{N}_2$  source, but the process offered minimal yields and low selectivity [41]. After several decades of progress, the yields from  $\text{TiO}_2$ -driven photosynthesis of  $\text{NH}_3$  have been enhanced by hundreds-fold [40]. However, most related studies still apply only UV light because of the narrow light absorption region of conventional  $\text{TiO}_2$ , which hinders the application range and produces low solar coulombic efficiency. As illustrated in Fig. 4a, by tracking the advanced  $\text{TiO}_2$  photocatalyst design milestones, it has high credits to investigate the  $\text{N}_2$  fixation to  $\text{NH}_3$  by taking phase-selective disordering and visible-light harvesting advantages of BTO for targeting maximized  $\text{NH}_3$  production yield and selectively under mild NPT conditions.

In recent years, volatile organic compounds (VOCs), which vaporize easily at room temperature, have become major hazardous pollutants in the air through speedy industrialization and urbanization. Some studies show that indoor atmospheres can have 2–10 times more VOCs than outdoor environments [42]. Therefore, VOCs' health concerns, such as cancer, headaches, and dizziness, are serious among people who spend most of their time in buildings or enclosed spaces. Among the various VOCs, toluene, benzene, and aldehydes (formaldehyde and acetaldehyde) are the most common and toxic species [43]. Photodegradation of VOCs is inevitably regarded as the best and most economical choice for dealing with VOCs in the air. The carbon–carbon bonding and carbonyl groups in VOC molecules are



comparatively stable, requiring sufficiently hot carriers from a powerful photocatalyst to be decomposed. BTO is expected to actively cause full VOC degradation into CO<sub>2</sub> and H<sub>2</sub>O by effectively generating photoinduced charges and inhibiting exciton recombination under solar and indoor LED lamplight (Fig. 4b). Additionally, the hydroxyl-rich character of the disordered portion of BTO can specifically support the covalent coating and binding process on various substrates and objects (such as air conditioner filters, indoor walls, and subway carriages) and thereby provide versatile application choices.

Microbial pathogens, which include various bacteria and viruses, are major health concerns to humans worldwide. They occasionally cause serious infectious disease pandemics, such as those caused by the novel coronavirus (COVID-19), severe acute respiratory syndrome

coronavirus (SARS), swine influenza virus (H1N1), and Middle-East respiratory syndrome coronavirus (MERS) [16]. For the sake of human health, society needs effective microbial disinfection systems with enough versatility to attack airborne, waterborne, and foodborne pathogenic species. Practically, various microbicidal processes have already been adopted, such as UV disinfection, antibiotic sterilization, thermal treatments, and nanofiltration. However, the current approaches possess significant limitations; for instance, some microbes have already evolved antibiotic or UV resistance [44], and thermal, and filtration operations can cause energy exhaustion and are incompatible in many spaces. The microbial pathogens inactivation by TiO<sub>2</sub> photocatalyst can trace to 1994 after the Sjogren et al. finds the inactivation ability to bacteriophage MS2 on TiO<sub>2</sub> [45]. Besides, TiO<sub>2</sub> could be a good option for

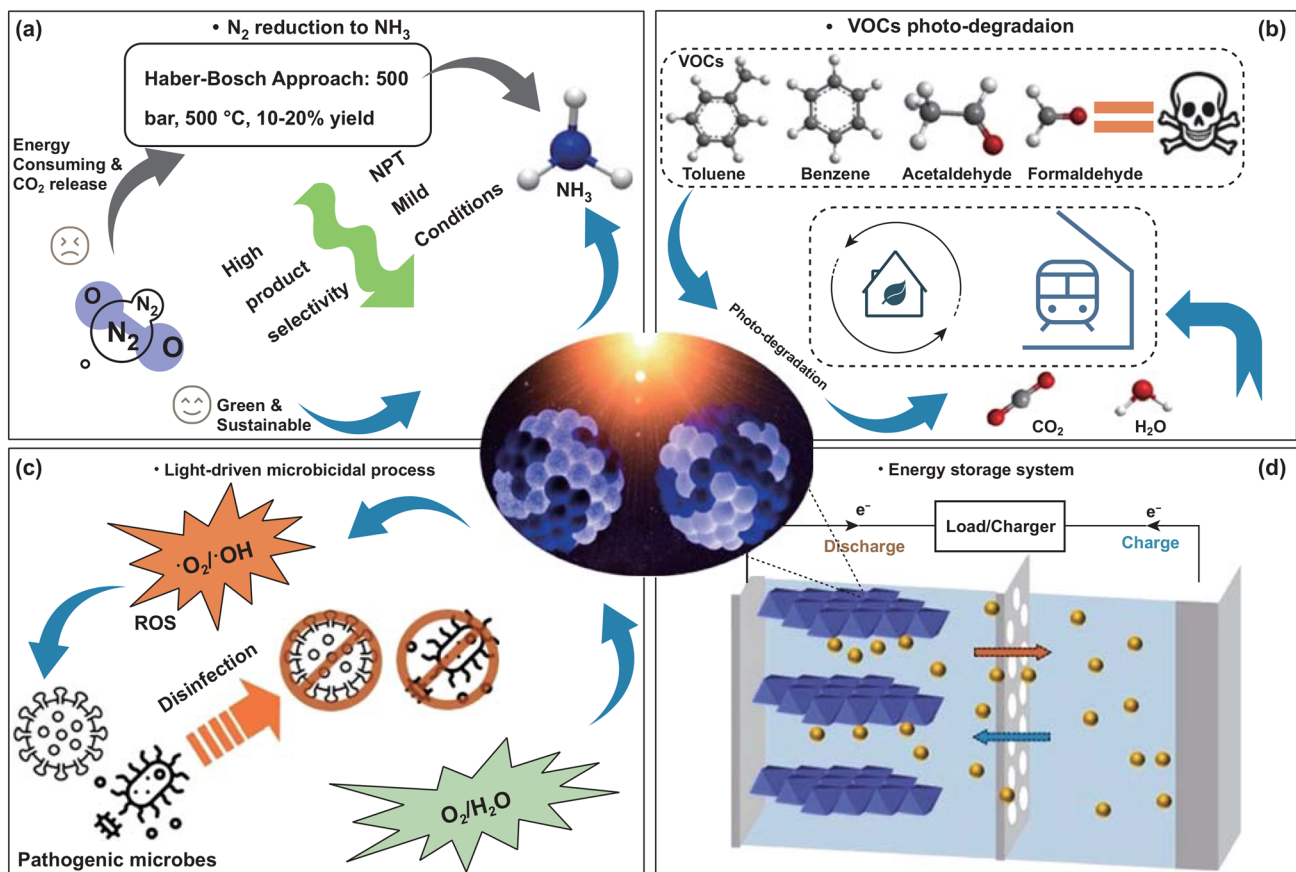


**Fig. 4** Potential applications and design commentary of BTO. **a** Photo-driven N<sub>2</sub> reduction to NH<sub>3</sub> to replace the conventional Haber–Bosch approach. **b** Photodegradation of volatile organic compounds (VOCs), especially in indoor atmospheres. **c** Adapting to visible-light-induced microbicidal processes. **d** Exploring BTO as electrode material in an energy storage system by taking advantage of its electro-conducting Ti<sup>3+</sup> species, oxygen vacancy, and stability

microorganism disinfection that is low cost, requires minimal energy consumption, and is harmless and eco-friendly [46, 47]. In the  $\text{TiO}_2$  photocatalysis microorganism disinfection process, the ROS generated from photocatalytic processes after light irradiation plays the major roles [16]. To further boost the microbial pathogens inactivation performance of  $\text{TiO}_2$ , we need to strengthen the producing amount of ROS species. In the authors' group previous reports, BTO can generate a higher amount of ROS species under UV, visible or solar light illumination, which is represented by the higher peak intensity of BTO than pristine  $\text{TiO}_2$  in electron paramagnetic resonance analysis [31, 48]. Therefore, BTO could act as a broad-spectrum antimicrobial agent and outperform pristine  $\text{TiO}_2$  by generating sufficient antibacterial and viricidal ROS at different band positions, as depicted in Fig. 4c. Harmful bacteria and viruses in living spaces could be effectively deactivated under mild conditions by using BTO and solar or visible light.

Because  $\text{TiO}_2$  has superior stability, high safety, and good economic value, it has been investigated and considered as an anode or cathode candidate in various ion battery systems, including single-valent alkali-ion batteries (LIBs, SIBs, and KIBs) [49], multivalent magnesium ion batteries (MIBs) [50] and aluminum ion batteries (AIBs) [51]. Also, researchers have noticed that  $\text{Ti}^{3+}$  self-doped black anatase  $\text{TiO}_2$  has better rate capability than pristine white anatase in LIBs [52], and the associated OV of black  $\text{TiO}_2$  resulted

in high-performance magnesium ion ( $\text{Mg}^{2+}$ ) storage [50]. Nevertheless, the synthesis of black  $\text{TiO}_2$  requires a high-temperature reduction process, and their black  $\text{TiO}_2$  products remain in a majority crystalline phase and only acquire a small portion  $\text{Ti}^{3+}$ ; even the OV and  $\text{Ti}^{3+}$  was suggested as main contributions to the advances. Therefore, we propose BTO (including the  $A_d$  and  $R_d$  synthesized by M-EDA) as an encouraging candidate for battery system electrodes (Fig. 4d). Our M-EDA reduction approach, along with the production of BTO under NPT conditions, can almost completely disorder anatase (Na-EDA) and rutile (Li-EDA)  $\text{TiO}_2$  and deliver sufficient OVs and electro-conducting  $\text{Ti}^{3+}$  species to enhance energy storage performance.

## 5 Prospects and Summary

The science and technology exploitation has been speeding up in modern society than any other historical era. Based on the invention of BTO, the research progress towards energy and society sustainability can be promoted from diverse aspects. The forthcoming flourishing research suggestions based on the account of BTO achievements are suggested below (Fig. 5).

1. Design and synthesize a BTO specific morphology and structure in a different dimension (0, 1, 2, 3D). Nano-structured materials are essential for photoelectrochemical devices because of their exposed active surfaces, obviously upgraded kinetics, and versatile adaptations

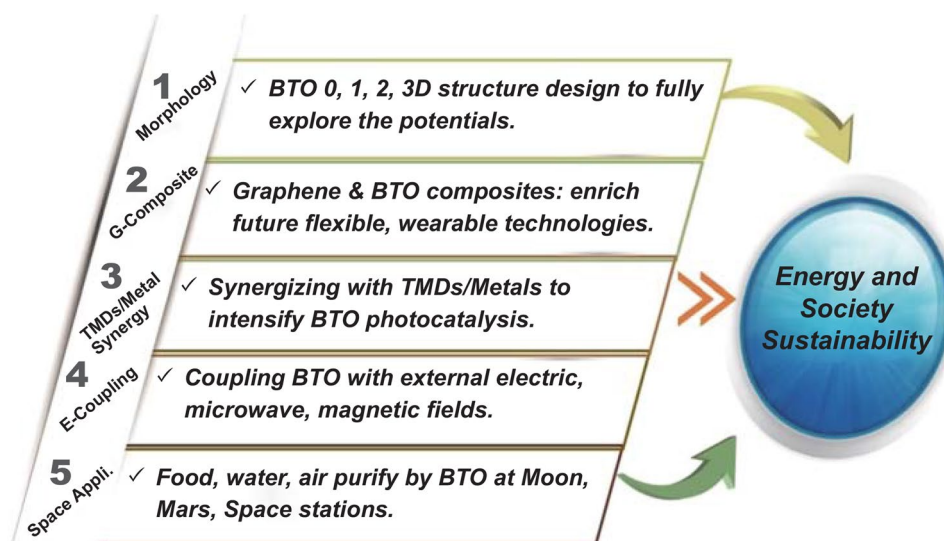


**Fig. 5** Future research suggestions based on the unique properties of BTO to improve energy and social sustainability

[53]. The potential of BTO could be widely explored by investigating it in 0D (quantum dots), 1D (nanowires, nanotubes, nanoribbons, and nanorods), 2D (nanoplates, nanodisks, and nanosheets), and 3D (nanoflowers, nano-coils, and ordered mesoporous framework) forms.

2. Construct graphene/carbon composites with BTO for use in flexible and wearable energy devices to advance their mechanical and electron flow properties.

3. Synergize BTO with other typical transition metal dichalcogenides and single or dual metal atoms to further boost its photocatalytic performance in terms of yield, selectivity, and long-term stability.

4. Couple BTO applications with external fields (electricity, magnetism, plasmonic energy, microwaves, or polarized light). The external fields are expected to influence the photocatalytic process in several ways, such as inducing polarization in reactant molecules (like CO<sub>2</sub>, N<sub>2</sub>, and VOCs) to assist in the dissociation of molecules, prompting chiral molecule pure enantiomer synthesis, and altering the hot carrier migration pathways of the photocatalyst under an electromagnetic wave, so on.

5. On the frontier of space science, one of the ultimate goals is to build an environment in which humans could live. Space applications of BTO could lead to a bright future for sustainable human civilization. Currently, the International Space Station is equipped with the “Photocatalytic Oxidation Reactor System” (PORS) for VOC removal during the potable water purification step [54]. And the Kennedy Space Center has developed a visible-light-responsive Ag-doped TiO<sub>2</sub> catalyst PORS in 2016 for better water purification system [55]. BTO, as an advanced photocatalyst, has shown superior photocatalytic activity than most noble metal-doped TiO<sub>2</sub> and will enable the efficient acquisition of clean-living necessities (food, water, and air) in the Space living area. Furthermore, researchers have found that up to 10 wt% of TiO<sub>2</sub> exists in the regional area of Moon’s crust, which can further serve to assist the future human exploration of the Moon [56].

Herein, we have described milestones in TiO<sub>2</sub> material design, including the development of BTO. Then, we explained our M-EDA phase-selective disordering mechanism and the unique advances offered by BTO in visible-light absorption and exciton disassociation. We continued by discussing applications already achieved and prospective advances from those. Last, we proposed several potential new prospects for BTO that target energy and social sustainability. Relying on the structure specialty and superior accomplishments, the unique NPT-synthesized

BTO could offer more socially beneficial applications and approach to commercial, robust visible-light-driven versatile photocatalyst if its potential is fully explored by the research community.

**Acknowledgements** This work was supported by the Institute for Basic Science (IBS-R011-D1) and partially supported by the Korea Evaluation Institute of Industrial Technology (20004627) and the INNOPOLIS Foundation (2019-DD-SB-0602).

**Open Access** This article is licensed under a Creative Commons Attribution 4.0 International License, which permits use, sharing, adaptation, distribution and reproduction in any medium or format, as long as you give appropriate credit to the original author(s) and the source, provide a link to the Creative Commons licence, and indicate if changes were made. The images or other third party material in this article are included in the article’s Creative Commons licence, unless indicated otherwise in a credit line to the material. If material is not included in the article’s Creative Commons licence and your intended use is not permitted by statutory regulation or exceeds the permitted use, you will need to obtain permission directly from the copyright holder. To view a copy of this licence, visit <http://creativecommons.org/licenses/by/4.0/>.

## References

1. E. Keidel, The fading of aniline dyes in the presence of titanium white. *Farben-Zeitung* **34**, 1242–1243 (1929)
2. A. Fujishima, K. Honda, S. Kikuchi, Photochemical reactions of semiconductors. I. Photosensitized electrolytic oxidation on semiconducting n-type TiO<sub>2</sub> electrode. *Kogyo Kagaku Zasshi* **72**(1), 108–113 (1969). <https://doi.org/10.1246/nikkaishi1898.72.108>
3. A. Fujishima, K. Honda, Electrochemical photolysis of water at a semiconductor electrode. *Nature* **238**(5358), 37–38 (1972). <https://doi.org/10.1038/238037a0>
4. F. Haque, T. Daenke, K. Kalantar-Zadeh, J.Z. Ou, Two-dimensional transition metal oxide and chalcogenide-based photocatalysts. *Nano-micro Lett.* **10**(2), 23 (2018). <https://doi.org/10.1007/s40820-017-0176-y>
5. D. Reyes-Coronado, G. Rodriguez-Gattorno, M.E. Espinosa-Pesqueira, C. Cab, R. de Coss et al., Phase-pure TiO<sub>2</sub> nanoparticles: anatase, brookite and rutile. *Nanotechnology* **19**(14), 145605 (2008). <https://doi.org/10.1088/0957-4484/19/14/145605>
6. K. Hashimoto, H. Irie, A. Fujishima, TiO<sub>2</sub> photocatalysis: a historical overview and future prospects. *Jpn. J. Appl. Phys.* **44**(12), 8269–8285 (2005). <https://doi.org/10.1143/jjap.44.8269>
7. T. Luttrell, S. Halpegamage, J. Tao, A. Kramer, E. Sutter et al., Why is anatase a better photocatalyst than rutile?—model studies on epitaxial TiO<sub>2</sub> films. *Sci. Rep.* **4**, 4043 (2014). <https://doi.org/10.1038/srep04043>



8. R.H. West, M.S. Celnik, O.R. Inderwildi, M. Kraft, G.J.O. Beran et al., Toward a comprehensive model of the synthesis of TiO<sub>2</sub> particles from TiCl<sub>4</sub>. *Angew. Ind. Eng. Chem. Res.* **46**(19), 6147–6156 (2007). <https://doi.org/10.1021/ie0706414>
9. S. Ngamta, N. Boonprakob, N. Wetchakun, K. Ounnunkad, S. Phanichphant et al., A facile synthesis of nanocrystalline anatase TiO<sub>2</sub> from TiOSO<sub>4</sub> aqueous solution. *Mater. Lett.* **105**, 76–79 (2013). <https://doi.org/10.1016/j.matlet.2013.04.064>
10. L. Qi, J. Yu, M. Jaroniec, Preparation and enhanced visible-light photocatalytic H<sub>2</sub>-production activity of CdS-sensitized Pt/TiO<sub>2</sub> nanosheets with exposed (001) facets. *Phys. Chem. Chem. Phys.* **13**(19), 8915–8923 (2011). <https://doi.org/10.1039/c1cp20079h>
11. Y. Ide, N. Inami, H. Hattori, K. Saito, M. Sohmiya et al., Remarkable charge separation and photocatalytic efficiency enhancement through interconnection of TiO<sub>2</sub> nanoparticles by hydrothermal treatment. *Angew. Chem. Int. Ed.* **55**(11), 3600–3605 (2016). <https://doi.org/10.1002/anie.201510000>
12. M. Moztahida, D.S. Lee, Photocatalytic degradation of methylene blue with P25/graphene/polyacrylamide hydrogels: optimization using response surface methodology. *J. Hazard. Mater.* **400**, 123314 (2020). <https://doi.org/10.1016/j.jhazmat.2020.123314>
13. B. Ohtani, O.O. Prieto-Mahaney, D. Li, R. Abe, What is degussa (evonik) P25? Crystalline composition analysis, reconstruction from isolated pure particles and photocatalytic activity test. *J. Photochem. Photobiol. A: Chem.* **216**(2–3), 179–182 (2010). <https://doi.org/10.1016/j.jphotochem.2010.07.024>
14. M.T. Noman, M.A. Ashraf, A. Ali, Synthesis and applications of nano-TiO<sub>2</sub>: a review. *Environ. Sci. Pollut. Res. Int.* **26**(4), 3262–3291 (2019). <https://doi.org/10.1007/s11356-018-3884-z>
15. A. Fujishima, X. Zhang, D. Tryk, TiO<sub>2</sub> photocatalysis and related surface phenomena. *Surf. Sci. Rep.* **63**(12), 515–582 (2008). <https://doi.org/10.1016/j.surfrep.2008.10.001>
16. A. Habibi-Yangjeh, S. Asadzadeh-Khaneghah, S. Feizpoor, A. Rouhi, Review on heterogeneous photocatalytic disinfection of waterborne, airborne, and foodborne viruses: can we win against pathogenic viruses? *J. Colloid. Interface Sci.* **580**, 503–514 (2020). <https://doi.org/10.1016/j.jcis.2020.07.047>
17. X. Chen, C. Burda, The electronic origin of the visible-light absorption properties of C-, N- and S-doped TiO<sub>2</sub> nanomaterials. *J. Am. Chem. Soc.* **130**(15), 5018–5019 (2008). <https://doi.org/10.1021/ja711023z>
18. S.N.R. Inturi, T. Boningari, M. Suidan, P.G. Smirniotis, Flame aerosol synthesized Cr incorporated TiO<sub>2</sub> for visible light photodegradation of gas phase acetonitrile. *J. Phys. Chem. C* **118**(1), 231–242 (2013). <https://doi.org/10.1021/jp404290g>
19. A. Ali, E. Yassitepe, I. Ruzybayev, S.I. Shah, A.S. Bhatti, Improvement of (004) texturing by slow growth of Nd doped TiO<sub>2</sub> films. *J. Appl. Phys.* **112**(11), 113505 (2012). <https://doi.org/10.1063/1.4767361>
20. X.B. Chen, L. Liu, P.Y. Yu, S.S. Mao, Increasing solar absorption for photocatalysis with black hydrogenated titanium dioxide nanocrystals. *Science* **331**, 746–750 (2011). <https://doi.org/10.1126/science.1200448>
21. L. Wang, K. Zhang, J.K. Kim, M. Ma, G. Veerappan et al., An order/disorder/water junction system for highly efficient co-catalyst-free photocatalytic hydrogen generation. *Energy. Environ. Sci.* **9**(2), 499–503 (2016). <https://doi.org/10.1039/c5ee03100a>
22. J. Pan, G. Liu, G.Q. Lu, H.M. Cheng, On the true photoreactivity order of {001}, {010}, and {101} facets of anatase TiO<sub>2</sub> crystals. *Angew. Chem. Int. Ed.* **50**(9), 2133–2137 (2011). <https://doi.org/10.1002/anie.201006057>
23. M. Xu, Y. Gao, E.M. Moreno, M. Kunst, M. Muhler et al., Photocatalytic activity of bulk TiO<sub>2</sub> anatase and rutile single crystals using infrared absorption spectroscopy. *Phys. Rev. Lett.* **106**(13), 138302 (2011). <https://doi.org/10.1103/PhysRevLett.106.138302>
24. D.C. Hurum, A.G. Agrios, K.A. Gray, T. Rajh, M.C. Thurnauer, Explaining the enhanced photocatalytic activity of degussa P25 mixed-phase TiO<sub>2</sub> using EPR. *J. Phys. Chem. B* **107**(19), 4545–4549 (2003). <https://doi.org/10.1021/jp0273934>
25. T. Ohno, K. Sarukawa, K. Tokieda, M. Matsumura, Morphology of a TiO<sub>2</sub> photocatalyst (degussa, P25) consisting of anatase and rutile crystalline phases. *J. Catal.* **203**(1), 82–86 (2001). <https://doi.org/10.1006/jcat.2001.3316>
26. X. Chen, L. Liu, F.Q. Huang, Black titanium dioxide (TiO<sub>2</sub>) nanomaterials. *Chem. Soc. Rev.* **44**(7), 1861–1885 (2015). <https://doi.org/10.1039/c4cs00330f>
27. A.J. Birch, 117. Reduction by dissolving metals. Part I. *J. Chem. Soc. (Resumed)*. (1944). <https://doi.org/10.1039/JR9440000430>
28. H.M. Hwang, S. Oh, J.-H. Shim, Y.-M. Kim, A. Kim et al., Phase-selective disordered anatase/ordered rutile interface system for visible-light-driven, metal-free CO<sub>2</sub> reduction. *ACS Appl. Mater. Interfaces* **11**(39), 35693–35701 (2019). <https://doi.org/10.1021/acsami.9b10837>
29. L.E. Oi, M.-Y. Choo, H.V. Lee, H.C. Ong, S.B.A. Hamid et al., Recent advances of titanium dioxide (TiO<sub>2</sub>) for green organic synthesis. *RSC Adv.* **6**(110), 108741–108754 (2016). <https://doi.org/10.1039/C6RA22894A>
30. J. Pal, T. Pal, Faceted metal and metal oxide nanoparticles: design, fabrication and catalysis. *Nanoscale* **7**(34), 14159–14190 (2015). <https://doi.org/10.1039/c5nr03395k>
31. Y. Kim, H.M. Hwang, L. Wang, I. Kim, Y. Yoon et al., Solar-light photocatalytic disinfection using crystalline/amorphous low energy bandgap reduced TiO<sub>2</sub>. *Sci. Rep.* **6**, 25212 (2016). <https://doi.org/10.1038/srep25212>
32. C.T.K. Nguyen, N.Q. Tran, S. Seo, H. Hwang, S. Oh et al., Highly efficient nanostructured metal-decorated hybrid semiconductors for solar conversion of CO<sub>2</sub> with almost complete CO selectivity. *Mater. Today* **35**, 25–33 (2020). <https://doi.org/10.1016/j.mattod.2019.11.005>
33. S. Bak, S.M. Lee, H.M. Hwang, H. Lee, Phase-selective modulation of TiO<sub>2</sub> for visible light-driven photocatalysis: tuning of absorption and adsorptivity. *Mol. Catal.* **471**, 71–76 (2019). <https://doi.org/10.1016/j.mcat.2019.04.017>

34. S. McAllister, J.Y. Chen, A.C. Fernandez-Pello, *Fundamentals of Combustion Processes* (Springer, New York, 2011), p. 244
35. G.D. Cooke, R.H. Kennedy, Managing drinking water supplies. *Lake Reserv. Manag.* **17**(3), 157–174 (2001). <https://doi.org/10.1080/07438140109354128>
36. X. Li, J. Yu, M. Jaroniec, X. Chen, Cocatalysts for selective photoreduction of CO<sub>2</sub> into solar fuels. *Chem. Rev.* **119**(6), 3962–4179 (2019). <https://doi.org/10.1021/acs.chemrev.8b00400>
37. A.L. da Silva, L. Wu, L.B. Caliman, R.H.R. Castro, A. Navrotsky et al., Energetics of CO<sub>2</sub> and H<sub>2</sub>O adsorption on alkaline earth metal doped TiO<sub>2</sub>. *Phys. Chem. Chem. Phys.* **22**(27), 15600–15607 (2020). <https://doi.org/10.1039/d0cp01787f>
38. X. Lang, X. Chen, J. Zhao, Heterogeneous visible light photocatalysis for selective organic transformations. *Chem. Soc. Rev.* **43**(1), 473–486 (2014). <https://doi.org/10.1039/c3cs60188a>
39. L. Wang, M. Xia, H. Wang, K. Huang, C. Qian et al., Greening ammonia toward the solar ammonia refinery. *Joule* **2**(6), 1055–1074 (2018). <https://doi.org/10.1016/j.joule.2018.04.017>
40. X. Xue, R. Chen, C. Yan, P. Zhao, Y. Hu et al., Review on photocatalytic and electrocatalytic artificial nitrogen fixation for ammonia synthesis at mild conditions: advances, challenges and perspectives. *Nano Res.* **12**(6), 1229–1249 (2019). <https://doi.org/10.1007/s12274-018-2268-5>
41. G.N. Schrauzer, T.D. Guth, Photolysis of water and photoreduction of nitrogen on titanium dioxide. *J. Am. Chem. Soc.* **99**(22), 7189–7193 (1977). <https://doi.org/10.1021/ja00464a015>
42. M. Stucchi, F. Galli, C.L. Bianchi, C. Pirola, D.C. Boffito et al., Simultaneous photodegradation of VOC mixture by TiO<sub>2</sub> powders. *Chemosphere* **193**, 198–206 (2018). <https://doi.org/10.1016/j.chemosphere.2017.11.003>
43. M.S. Kamal, S.A. Razzak, M.M. Hossain, Catalytic oxidation of volatile organic compounds (VOCs)—a review. *Atmos. Environ.* **140**, 117–134 (2016). <https://doi.org/10.1016/j.atmosenv.2016.05.031>
44. D. Li, A.Z. Gu, M. He, H.C. Shi, W. Yang, UV inactivation and resistance of rotavirus evaluated by integrated cell culture and real-time RT-PCR assay. *Water Res.* **43**(13), 3261–3269 (2009). <https://doi.org/10.1016/j.watres.2009.03.044>
45. J.C. Sjogren, R.A. Sierka, Inactivation of phage MS<sub>2</sub> by iron-aided titanium dioxide photocatalysis. *Appl. Environ. Microbiol.* **60**(1), 344 (1994)
46. M. Liu, K. Sunada, K. Hashimoto, M. Miyauchi, Visible-light sensitive Cu(ii)-TiO<sub>2</sub> with sustained anti-viral activity for efficient indoor environmental remediation. *J. Mater. Chem. A* **3**(33), 17312–17319 (2015). <https://doi.org/10.1039/c5ta03756e>
47. R. Nakano, M. Hara, H. Ishiguro, Y. Yao, T. Ochiai et al., Broad spectrum microbicidal activity of photocatalysis by TiO<sub>2</sub>. *Catalysts* **3**(1), 310–323 (2013). <https://doi.org/10.3390/catal3010310>
48. Y. Luo, L. Wang, Y. Hwang, J. Yu, J. Lee et al., Binder-free TiO<sub>2</sub> hydrophilic film covalently coated by microwave treatment. *Mater. Chem. Phys.* **258**, 123884 (2021). <https://doi.org/10.1016/j.matchemphys.2020.123884>
49. J. Yang, X. Xiao, W. Gong, L. Zhao, G. Li et al., Size-independent fast ion intercalation in two-dimensional titania nanosheets for alkali-metal-ion batteries. *Angew. Chem. Int. Ed.* **58**(26), 8740–8745 (2019). <https://doi.org/10.1002/anie.201902478>
50. Y. Wang, X. Xue, P. Liu, C. Wang, X. Yi et al., Atomic substitution enabled synthesis of vacancy-rich two-dimensional black TiO<sub>2-x</sub> nanoflakes for high-performance rechargeable magnesium batteries. *ACS Nano* **12**(12), 12492–12502 (2018). <https://doi.org/10.1021/acs.nano.8b06917>
51. S. Wang, K.V. Kravchyk, S. Pigeot-Rémy, W. Tang, F. Krumeich et al., Anatase TiO<sub>2</sub> nanorods as cathode materials for aluminum-ion batteries. *ACS Appl. Nano Mater.* **2**(10), 6428–6435 (2019). <https://doi.org/10.1021/acsanm.9b01391>
52. S.-T. Myung, M. Kikuchi, C.S. Yoon, H. Yashiro, S.-J. Kim et al., Black anatase titania enabling ultra high cycling rates for rechargeable lithium batteries. *Energ. Environ. Sci.* **6**(9), 2609 (2013). <https://doi.org/10.1039/c3ee41960f>
53. J.N. Tiwari, R.N. Tiwari, K.S. Kim, Zero-dimensional, one-dimensional, two-dimensional and three-dimensional nanostructured materials for advanced electrochemical energy devices. *Prog. Mater. Sci.* **57**(4), 724–803 (2012). <https://doi.org/10.1016/j.pmatsci.2011.08.003>
54. M. P. Nagaraja, Water on the space station. (NASA Science Share the Science, 2000). [https://science.nasa.gov/science-news/science-atnasa/2000/ast02nov\\_1](https://science.nasa.gov/science-news/science-atnasa/2000/ast02nov_1). Accessed 5 Nov 2020
55. J.L. Coutts, P.E. Hintze, A. Meier, M.G. Shah, R.W. Devor et al., Visible-light-responsive photocatalysis: ag-doped TiO<sub>2</sub> catalyst development and reactor design testing. 46th International conference on environmental systems. 169 (2016)
56. M.S. Robinson, B.W. Hapke, J.B. Garvin, D. Skillman, J.F. Bell et al., High resolution mapping of TiO<sub>2</sub> abundances on the moon using the hubble space telescope. *Geophys. Res. Lett.* **34**(13), L13203 (2007). <https://doi.org/10.1029/2007gl029754>

